Tunable Submillimeter Interferometers of the Fabry-Perot Type*

R. ULRICH†, MEMBER, IEEE, K. F. RENK†, AND L. GENZEL†

Summary—Fabry-Perot Interferometers (FPI's) have been constructed for the far infrared and submillimeter wave region with metal grids as reflectors. Two-dimensional grids with square holes (metallic mesh) can be used for unpolarized radiation, too, and they are more convenient for the construction than one-dimensional (parallel wire) grids. The performance of several FPI's has been measured in the 100–600 μ wavelength region. Q values in first-order range from 5 to 30, and peak transmissions up to 0.9 have been reached. The experimental results are in qualitative agreement with the theory of thin parallel wire gratings. The influence of the unevenness of the reflectors is studied theoretically. Applications of a submillimeter FPI include its use as the dispersion element in a spectrometer, as a narrow-band filter to check the radiation purity of a grating spectrometer, and as a separator of the harmonics from a crystal harmonic generator.

I. Introduction

THE REALIZATION of a FPI for the infrared depends on finding the proper reflectors for this spectral region. The required optical properties of the reflectors follow from the Airy formula (1) for the FPI: the power transmissivity $\tau(\lambda)$ of a FPI with two identical, plane, and parallel reflectors for a normally incident plane wave of wavelength λ is

$$\tau(\lambda) = \left(1 - \frac{A}{1-R}\right)^2 \cdot \left(1 + \frac{4R}{(1-R)^2}\sin^2 \delta/2\right)^{-1} \quad (1)$$

where

$$\delta = 4\pi nd/\lambda - 2(\phi - \pi), \quad (2)$$

and where $R^{1/2} \cdot e^{i\phi}$ is the amplitude reflection coefficient of the single reflector. A is its power absorptivity, d is the distance of the two reflectors, and n is the refractive index of the lossless medium between them. The FPI has its maximal transmission

$$\tau_0 = \left(1 - \frac{A}{1-R}\right)^2 = \left(1 + \frac{A}{T}\right)^{-2} \quad (3)$$

in qth order at the wavelength λ_q which is obtained from $\delta = 2\pi q$ with $q = 1, 2, 3, \cdots$. The power transmissivity of the single reflector is $T = 1 - R - A$. The resolving power Q is defined with the half-value width $\Delta\lambda$ of the FPI transmission band centered at λ_q,

$$Q = \lambda_q/\Delta\lambda = q \cdot F. \quad (4)$$

F is called "finesse" and the Q value in first order. From (1)

$$F = \pi \Big/ \left(2 \arcsin \frac{1-R}{2R^{1/2}}\right) \simeq \frac{\pi R^{1/2}}{1-R}. \quad (5)$$

The approximation is valid to better than 3 per cent for $R \geq 0.6$. The quantities A, R, T, ϕ, Q and F depend on the wavelength, but they are assumed to be essentially constant within $\Delta\lambda$.

For most applications one is interested in obtaining a certain, usually high, value of Q in an order as low as possible. At the same time the peak transmission τ_0 should be sufficiently high. These demands of a high $Q/q = F$ and a high τ_0 determine by (3) and (5) the optical properties necessary for the reflectors of an FPI,

$$A \ll (1 - R) \quad \text{and} \quad (1 - R) \ll 1. \quad (6)$$

These requirements cannot be fulfilled simultaneously by thin homogeneous metal layers in the far infrared.[1] This is in contrast to the visible spectral region. Metal grids or perforated plates are known as reflectors in microwave FPI's,[2–4] and Q values up to 10^5 have been reported. These reflectors can be scaled down to far infrared wavelengths. They still, fulfill (6) and theoretically Q values of a similar order of magnitude are possible. In the far infrared, however, such high Q's cannot yet be utilized because of the low spectral power density of the available radiation sources. Therefore, we had to work only in the lowest orders of interference ($q \leq 15$). Similarly, the involved distances d are so small (<2 mm) that diffraction effects due to the finite size of the actual reflectors are negligible and the simple Airy theory (1) is applicable.

II. Properties of Metal Grids

Two types of grids will be considered. The one-dimensional (1d) grid of parallel wires of circular or rectangular cross section and the two-dimensional (2d)

* Received January 21, 1963; revised manuscript received June 18, 1963. This paper was presented in a shorted version, under the title, "Far Infrared Fabry-Perot Interferometers and Their Applications," at the Millimeter and Submillimeter Wave Conference, Orlando Fla., January, 1963. The paper is an extension of a previous work of K. F. Renk and L. Genzel, "Interference filters and Fabry-Perot interferometers for the far infrared," *J. Appl. Phys.*, vol. 1, pp. 643–648; September, 1962.

† Physikalisches Institut der Universitaet, 78 Freiburg im Breisgau, Germany.

[1] L. N. Hadley and D. M. Dennison, "Reflection and transmission interference filters," *J. Opt. Soc. Am.*, vol. 37, pp. 451–465; June, 1947.

[2] E. A. Lewis and J. P. Casey, "Metal grid interference filters," *J. Opt. Soc. Am.*, vol. 41, p. 360; 1951.

[3] G. v. Trentini, "Maximum transmission through a pair of wire gratings," *J. Opt. Soc. Am.*, vol. 45, pp. 883–885; October, 1955.

[4] W. Culshaw, "High resolution millimeter wave Fabry-Perot interferometer," IRE TRANS. ON MICROWAVE THEORY AND TECHNIQUES, vol. MTT-8, pp. 182–189; March, 1960.

grid or metallic mesh (Fig. 1). For the application to a FPI the grids shall act only as reflectors for nearly normally incident radiation. In order to avoid diffraction sidewaves the grating constant g must be smaller than the wavelengths involved,

$$\lambda/g > 1.$$

A. The 1d Grid

In the region $\lambda/g > 1$ the properties of the 1d grid are well known theoretically and experimentally.[5-9] The 1d grid is nearly completely transparent for radiation polarized with the electric vector perpendicularly to the wires ("capacitive grid," see Marcuvitz[7]). Parallel polarized radiation is partially transmitted and partially reflected ("inductive grid"[7]). The equivalent circuit representation of the thin 1d inductive grid with negligible absorption is given in Fig. 2(a). An infinite transmission line of characteristic impedance Z_0 shunted with a reactance jX_0. All theories of the 1d grid[5,7,8] show that for $\lambda \gg g$,

$$X_0/Z_0 = wg/\lambda \tag{7}$$

where the factor w depends only on the cross section of the wires. For $a \ll g$ (Fig. 1) is

for circular wires of radius a: $w = \ln (g/2\pi a)$,

for flat strips of breadth $2a$: $w = \ln \csc (\pi a/g)$.

Marcuvitz[7] also considers wires of elliptical and rectangular cross sections. The phase of the amplitude reflection coefficient is, from Fig. 2(a),

$$\phi = \pi - \arctan 2X_0/Z_0 \tag{8}$$

if the time periodicity is $e^{+j\omega t}$. The transmissivity T and reflectivity R of the inductive grid are

$$T = 1 - R = \sin^2 \phi \simeq \tan^2 \phi = 4w^2g^2/\lambda^2. \tag{9}$$

The approximation is valid for $\lambda \gg g$ so that $\phi \to \pi$.

The absorption A has been neglected up to now, but can be easily calculated for the inductive grid if the current distribution may be assumed to be uniform along the circumference of the wires, *i.e.*, for thin wires and an even smaller skin depth s. This condition $s \ll a \ll g$ is considered to be sufficiently satisfied in the far infrared when $g/a \geq 8$ and $\lambda \gg g$. The currents in the wires follow from the change of the magnetic field across the grid, and the ratio of the dissipated to the incident radiation yields

$$A = \frac{cgR}{\pi u \sigma s} = \frac{2g}{u} \cdot R \cdot \left(\frac{c}{\sigma\lambda}\right)^{1/2}. \tag{10}$$

Here u is the circumference of the wires which may have arbitrary cross sections. For circular wires $u = 2\pi a$ and (10) becomes identical with the absorptivity found by Casey and Lewis.[8] In the equivalent circuit the absorption may be represented by an additional impedance $(1+j)sg\pi Z_0/(u \cdot \lambda)$ in series with jX_0. Its influence is to decrease R and to increase T.[10] A numerical example follows. For a grid of round copper wires, $\lambda = 200\ \mu$, $R = 0.88$, and $g/a = 8$, (10) gives $A \simeq 0.4$ per cent. The changes in R and T are of the same order of magnitude. This low absorptivity and the high reflectivity at $\lambda \gg g$ make possible the construction of FPI's for the submillimeter region with high peak transmissions and a finesse comparable to that obtained in the visible by metal layer FPI's. With the figures of the example just mentioned, $\tau_0 \simeq 0.94$ and $F \simeq 25$ follow from (3) and (5). A FPI with 1d grids works, however, only for radiation polarized parallel to the wires.

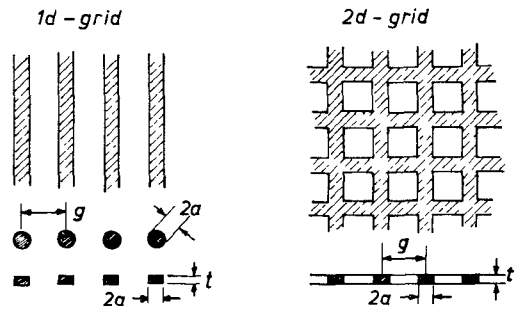

Fig. 1—The one-dimensional and the two-dimensional grid.

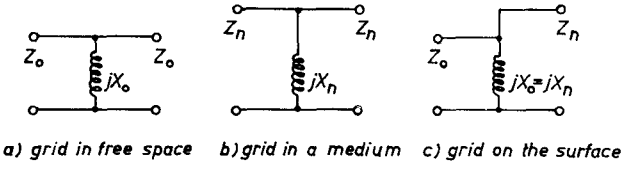

Fig. 2—Transmission of metal grids.

B. The 2d Grid

A reflector that is insensitive to polarization at normal incidence is the 2d grid if it has square symmetry. Thus, a FPI with 2d grids can transmit twice the energy of a 1d FPI from an unpolarized radiation source as the mercury arc. 2d grids are also preferable for far infrared FPI's because they are more readily available (electroformed metallic mesh with g down to about 10 microns) and are more convenient to handle than equivalent 1d grids.

[5] T. Larsen, "A survey of the theory of wire grids," IRE TRANS. ON MICROWAVE THEORY AND TECHNIQUES, vol. MTT-10, pp. 191–201; May, 1962.

[6] H. Lamb, "On the diffraction in transmission of electric waves by a metallic grating," *Proc. London Math. Soc.*, vol. 29, p. 528; 1898.

[7] N. Marcuvitz, "Waveguide Handbook," M.I.T. Rad .Lab. Ser., McGraw-Hill Book Company, Inc., New York, N. Y. no. 10, p. 280; 1951.

[8] J. P. Casey and E. A. Lewis, "Interferometer action of a parallel pair of wire gratings," *J. Opt. Soc. Am.*, vol. 42, pp. 971–977; December, 1952.

[9] W. K. Pursley "The Transmission of Electromagnetic Waves Through Wire Diffraction Gratings," Ph.D. dissertation, The University of Michigan, Ann Arbor; 1956.

[10] This can be seen from a discussion of eq. (20) of Casey and Lewis.[8]

In contrast to the 1d grids only few details are known about the optical properties of 2d grids. Their independence of the polarization at normal incidence follows from symmetry. An arbitrarily polarized wave incident on the grid may be decomposed into two components polarized parallel to the two main directions of the grid. Because of the symmetry both components are transmitted in the same manner, and they add behind the grid to a wave of the same polarization as the incident wave. An equivalent consideration applies to the reflected wave.

The optical properties of the 2d grid for $\lambda > g$ may be qualitatively derived from the known properties of 1d grids. The 2d grid is thought to be made up of two independent 1d grids which are laid across each other. Then each of the above-mentioned components of polarization "sees" an inductive and a capacitive grid. At $\lambda \gg g$ the latter may be assumed to be completely transparent, and each component is only affected by a 1d-inductive grid. Thus a 2d-metal grid should qualitatively act for any polarization as one of its composing 1d grids acts for parallel polarized radiation. Quantitative agreement is to be expected in the limit of very thin wires $a \ll g$.

This comparison of the 2d- and the 1d-inductive grid has been confirmed by our measurements on 2d grids. Fig. 3 shows in the reduced scale λ/g the transmission of a 2d grid ($g = 50\,\mu$, $g/a = 8$, $t = a$) measured from 40-μ to 290-μ wavelength. For $\lambda/g \geq 2$ the measured transmissivity may be described by the approximate form of (9), $T = w^2 g^2/\lambda^2$ with $w = 0.70$. Only a difference of the order of the errors of the measurement was found between the transmissivity of a copper and a nickel grid of equal dimensions. For comparison, in Fig. 3 the transmissivity of a 1d-inductive grid is given which was measured with microwaves ($\lambda = 3$ cm, $g/a = 8$, $t \simeq 0$) by Pursley.[9] Both types of grids show the same general behavior. The maximum of the transmission curve is, however, shifted from $\lambda = g$ (thin 1d grid) to a longer wavelength $\lambda = 1.15g$ (2d grid). We could not explain this effect definitely. It may be due to the considerable thickness of our 2d grids ($t = a$). This possibility is indicated by the two calculated transmission curves in Fig. 3. They were obtained from the theory of Marcuvitz[7] for 1d grids of rectangular wires. The transmissivity of the thick grid exceeds that of the thin grid in the region $g < \lambda < 1.4g$, and reaches $T = 0.99$ at $\lambda = 1.15g$.

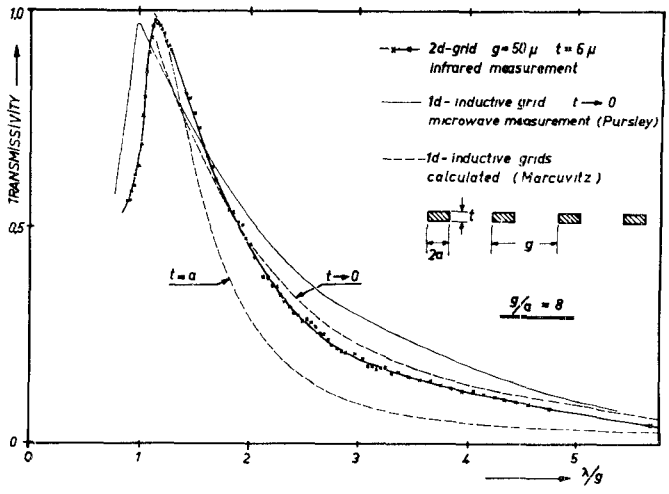

Fig. 3—Equivalent circuits for thin inductive metal grids.

C. The Metal Grid on the Surface of a Dielectric Medium

In some construction of FPI's the reflector grids were glued to the surface of dielectric plates. The presence of the dielectric has some influence on the optical properties of the grids, but the action of the FPI may still be described by (1)–(6) if a modified reflectivity R' and transmissivity T' are inserted. They can be calculated approximately for $\lambda \gg g$ if absorption is neglected. First a grid is considered which is completely embedded in a dielectric medium (relative permittivity $\epsilon = n^2$, relative permeability $\mu = 1$, normalized impedance $Z_n/Z_0 = 1/n$, wavelength in the medium $\lambda_n = \lambda_0/n$, in vacuum λ_0). The wave equation for the spatial part E of the electric field at the grid $\Delta E + (2\pi/\lambda_n)^2 E = 0$ and the boundary conditions do not explicitly contain n. Thus, their solutions are only determined by λ_n and the geometry of the grid. The impedance of the grid, normalized with respect to the impedance of the surrounding medium, is therefore given by the same function (7) as for a grid in free space, but with λ_n instead of λ_0,

$$X_n/Z_n = wg/\lambda_n.$$

From this follows

$$X_n = X_0 = Z_0 \cdot wg/\lambda_0.$$

This absolute impedance of the grid is independent of n in the approximation of (7) and is, therefore, the same for a grid inside and outside the medium. If it is assumed to remain also unchanged if the grid is at the surface of the medium, the properties R' and T' for the grid at the surface of the dielectric may be calculated from the equivalent circuit of Fig. 2(c),

$$\frac{T'}{T} = \frac{1 - R'}{1 - R} = \frac{n}{R + (n+1)^2 T/4}. \qquad (11)$$

Here R and T are the values for the grid in free space. Thus, the presence of the dielectric medium increases the transmissivity of the inductive grid. This theoretical result has been confirmed experimentally. At $\lambda = 200\,\mu$ the transmissivity of the 2d grid from Fig. 3 is increased by a factor $T'/T = 1.77 \pm 0.05$ when the grid is glued to the surface of a plate of crystal quartz ($n = 2.12$).[11] The absorption of the quartz and reflections from the second surface of the quartz plate have been taken into ac-

[11] R. Geick, "Der Brechungsindex von kristallinem und geschmolzenem Quarz im Spektralbereich um 100 μ," *Z Phys.*, vol. 161, pp. 116–122; December, 1961.

count. The agreement with the result of (11), $T'/T = 1.81$, is within the errors of the measurement.

The optical properties of an inductive grid at the interface between two dielectric media (n_1, n_2) may be obtained for $\lambda \gg g$ by a similar consideration,

$$T' = 1 - R' = T \frac{n_1 n_2}{R + (n_1 + n_2)^2 T/4} \cdot \qquad (11a)$$

III. Theoretical Properties of FPI with Metal Grids

The properties which are to be expected for a FPI with 2d grids follow directly from the considerations in Sections I and II if $\lambda \gg g$ and the approximation in (9) is applicable.

The wavelengths λ_q of maximal transmission are

$$\lambda_q = 2(nd + wg/\pi)/q \qquad q = 1, 2, 3 \cdots . \qquad (12)$$

The term wg/π arises from the fact that the change of phase connected with each reflection at the grid is not exactly π. The action of the inductive grid is equivalent to a reflection with exactly $\phi = \pi$ but at a plane which is located at a distance $wg/2\pi$ behind the grid. As the position of this plane is independent of the wavelength the frequencies corresponding to λ_q lie harmonically.

The theoretical finesse of a FPI of two grids in free space is found from (5) and (9), neglecting absorption

$$F = \frac{\lambda^2 \pi}{4w^2 g^2} (1 + 4w^2 g^2/\lambda^2)^{1/2} \simeq \lambda^2 \cdot \frac{\pi}{4w^2 g^2} \cdot \qquad (13)$$

The approximation is valid if $\lambda \gg g$. Concerning the finesse of a FPI with the grids on the surface of a dielectric, (11) must also be regarded, and

$$F' \simeq \frac{\lambda^2}{n} \cdot \frac{\pi}{4w^2 g^2} \qquad (13a)$$

in the same approximation as (13). At long wavelengths both F and F' become proportional to λ^2.

The peak transmission of the FPI with 2d grids is calculated assuming the same absorptivity (10) for the 2d as for the 1d-inductive grid. This is reasonable if $g/a \gg 1$,

$$\tau_0 = \left(1 + \frac{A}{T}\right)^{-2} \simeq 1 - \frac{\lambda^{3/2}}{6agw^2(c/\sigma)^{1/2}} \cdot \qquad (14)$$

For the FPI, with the grids on the surface of a dielectric, T' from (12) instead of T must be used and a similar expression results.

These theoretical values will be compared with the experimental λ_q, F and τ_0 in Section V.

IV. Design of the FPI's

The main problem in the construction of the FPI's is to keep the very thin grids ($t = 6$ microns) as plane as possible and parallel to each other. The absolute deviations Δd in spacing due to unevenness and poor parallelism must be sufficiently small ($\Delta d \ll \lambda/(4nF)$, see Appendix, if they shall not affect the performance of the FPI. With $\lambda = 200$ μ, $n = 1$, $F = 25$, for example, $\Delta d \ll 2$ μ is necessary. The parallelism must be adjustable for the same reason to some seconds of arc.

Several constructions with fixed and with variable spacing have been tried.

1) The simplest way to keep the grids plane was to glue them to plates of crystal quartz (parts 5 and 6 in Fig. 4). These plates have surfaces worked plane to optical quality and they are sufficiently transparent to the infrared radiation. They are attached to the two rings 1 and 2. The grids are glued with collodion to their inner surfaces. Their distance can be varied by means of the thread 3 from zero to several millimeters. Thus, the FPI is tunable. Three springs 4 prevent backlash, and the screws 8 serve for the adjustment of the parallelism of the grids. It can be checked by illuminating the plates with monochromatic visible light and observing the Haidinger fringes due to reflections between the inner surfaces of the plates. The diameter of the usable area of the FPI is 6 cm.

2) A FPI with fixed spacing can be made up of two 2d grids which are glued to both sides of a foil of polyethylene. The advantages of this construction are its simplicity and sturdiness. The foil need not be extremely plane, only a uniform thickness is necessary.

3) In the construction of Fig. 5 and Fig. 6, the grids have no substrate which may affect their optical properties or introduce additional absorption. The grids G_1, G_2 are glued to the frames 2, 4 and are stretched like a drumskin over the rings 6 by means of three screws 7. These rings are of glass. Their surfaces adjacent to the grids are optically plane and silvered semitransparently. Thus, the parallelism of the grids may be checked by observing the interference pattern through the rings as in the construction Fig. 4. In order to adjust the grids parallel, the frame 4 can be tilted by 9 with respect to the frame 3. A similar adjustment (not drawn in Fig. 5) is provided perpendicularly to the first one to tilt 3 with respect to the base plate 1. The spacing between the grids can be varied in a measurable way by the micrometer screw M. The parallelism is maintained by two equal foil springs 5. This arrangement is similar to a construction of Greenler[12] for the near infrared.

The transmissivity of the FPI's was measured in a grating spectrometer which has been described in detail by Genzel and Eckhardt.[13] The radiation source is a mercury arc lamp, and the receiver is a metal film bolometer at room temperature. The spectrometer may be evacuated in order to avoid the absorption of the atmospheric water vapor.

[12] R. G. Greenler, "Un Spectromètre Interferentiel Fabry-Pérot pour l'Infra-Rouge," Colloque international sur les progrès récents en spectroscopie interférentielle, Seine-et-Oise, France; 1959.

[13] L. Genzel and W. Eckhardt, "Spektraluntersuchungen im Gebiet um 1 mm Wellenlänge, I. Konstruktion des Spektrometers," *Z. Phys.*, vol. 139, pp. 578–591; December, 1954.

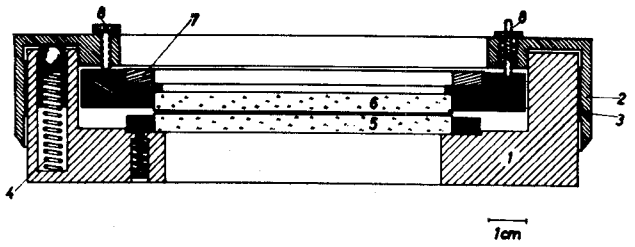

Fig. 4—Construction of a FPI: 2d grids on plates of crystal quartz.

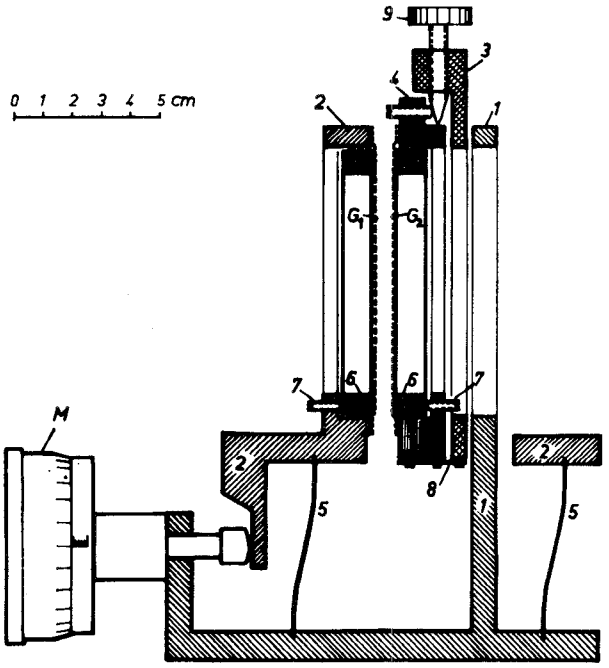

Fig. 5—Construction of a FPI: 2d grids without substrate.

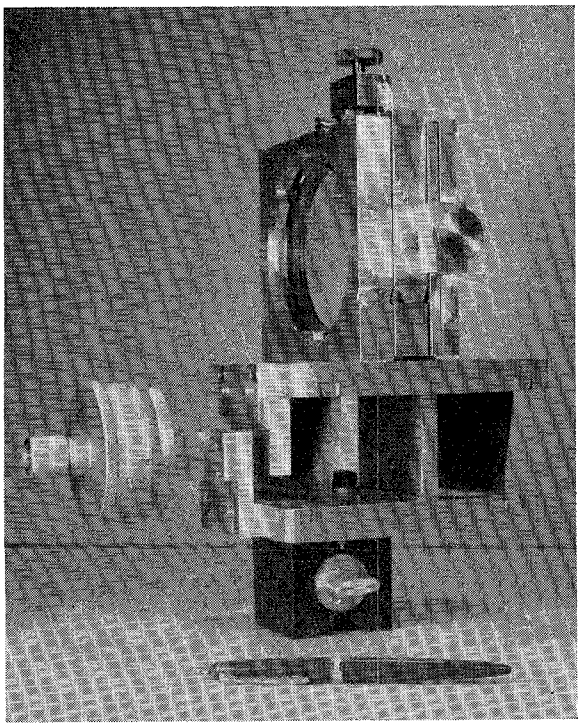

Fig. 6—Photograph of a FPI: 2d grids without substrate.

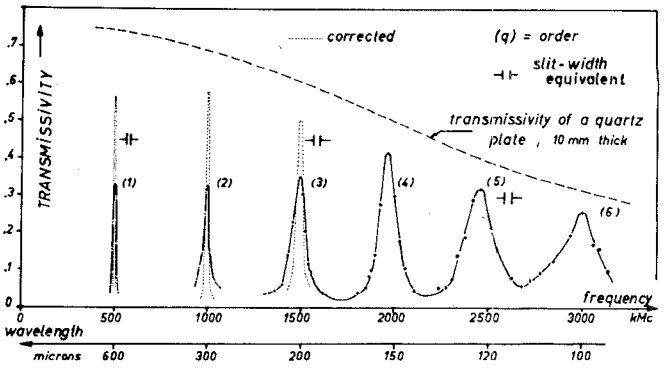

Fig. 7—Measured transmission of a FPI (2d grids on plates of crystal quartz).

At wavelengths $\lambda \geq 400\,\mu$ the resolution of the FPI's, especially in higher orders, became comparable to that of the spectrometer. Therefore, the measured transmission curves had to be corrected to zero-slit width.[14] Another slight correction was necessary at the longest wavelengths for the fact that the FPI's were measured in a convergent, rather than in a parallel, beam (aperture $\simeq 9°$).[15] These corrections are indicated by the dotted lines in Fig. 7.

V. Experimental Results

Fig. 7 is an example of a measured transmission characterisitic of a FPI. It was obtained with the FPI described in Section IV, 1) at a fixed spacing of approximately 300 μ. The first through sixth order lie harmonically on the frequency scale. An exact comparison with (12) and the determination of ϕ were, however, not possible because of difficulties in measuring the spacing d with sufficient accuracy.

Transmission curves like Fig. 7 have been recorded for a number of different spacings. From the half width of the transmission bands of the lowest orders the finesse $F = Q/q$ could be determined as a function of the wavelength. In Fig. 8 these results and the corresponding peak transmissions are compared with the theoretical expectations for this construction. The theoretical finesse was calculated using (5) and (11) with $w = 0.70$ from the measurements on single grids. For $\lambda = 200\,\mu$ the approximation (13a) is sufficient. The experimental finesse shows the nearly square dependence on wavelength indicated by (13a), but it remains smaller than the theoretical F'. The same is true for τ_0. The experimental values range from 26 per cent to 60 per cent including the reflection losses at the outer surfaces of the quartz plates and the absorption in the 10-mm quartz. These losses are recognizable in Fig. 7. The broken line represents the transmissivity of a 10-mm thick plate of crystal quartz. It was calculated from measurements of

[14] G. Koppelmann and K. Krebs, "Die optischen Eigenschaften von Interferenzfiltern bei Messung mit endlich breiten Spalten," *Z. Phys.*, vol. 157, p. 592; 1960.

[15] G. Koppelmann and K. Krebs, "Mehrstrahlinterferenzen in konvergentem Licht," *Z. Phys.*, vol. 158, pp. 172–180; February, 1960.

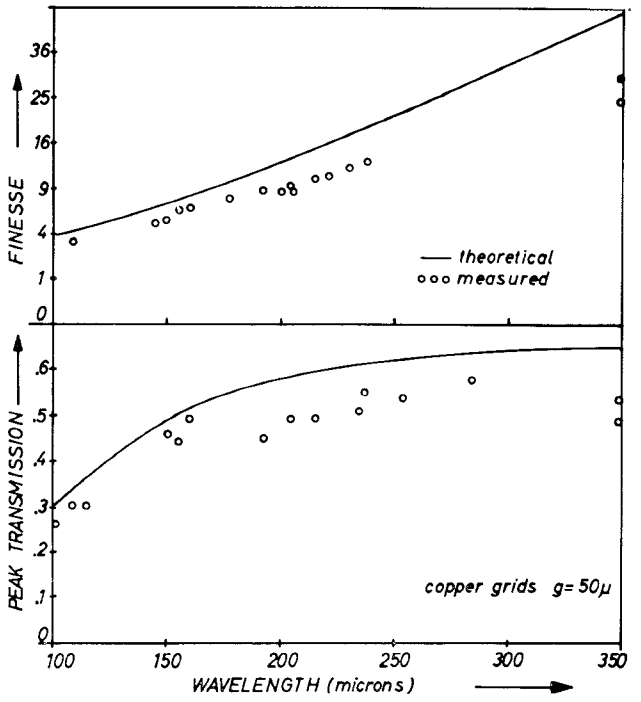

Fig. 8—Properties of a FPI (2d grids on plates of crystal quartz, Fig. 4).

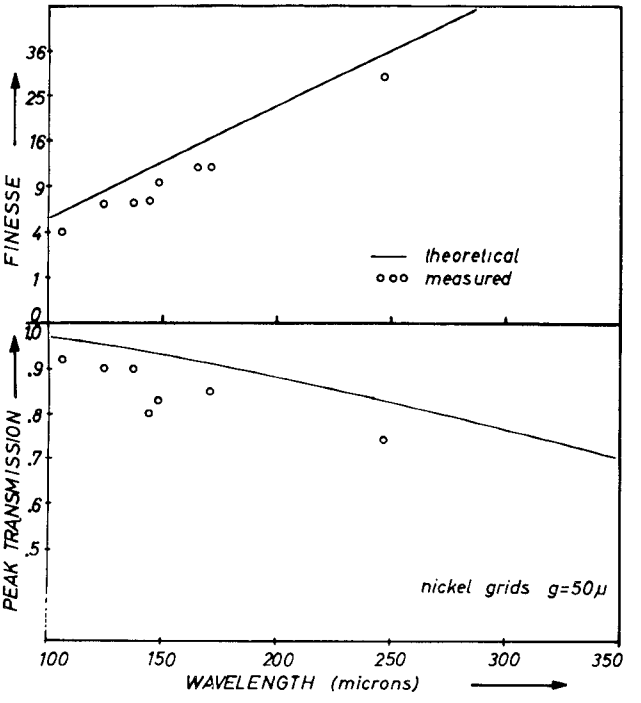

Fig. 9—Properties of a FPI: 2d grids without substrate.

Geick[11] for a plate cut perpendicularly to the optical axis. The product of this transmissivity of quartz with that calculated from (3), (9), (10), and (11) is the theoretical curve in Fig. 8. Also for τ_0 the experimental points show the expected general dependence on wavelength. They lie, however, below the theoretical curve by approximately the same factor as the F' values do. This fact indicates that the discrepancy between theoretical and experimental values is caused by the unevenness of the grids and perhaps by an insufficient parallelism (see Appendix).

The properties of the FPI were found to be independent of an in-plane rotation of one grid with respect to the other. Thus, the 2d grids do not show polarization effects at normal incidence. This was expected from their square symmetry.

Several FPI's of the simple type, Section IV, 2) were made with foils of polyethylene, 50 μ-thick, $n=1.5$. The first-order transmission bands lie at $\lambda\simeq 195\ \mu$. This is consistent with (12) if 2 microns are admitted for the thickness of each layer of glue (collodion). The measured finesse was $F\simeq 10$ for all specimens and $\tau_0\simeq 40$ per cent. The theoretical values are $F=15$ and $\tau_0=89$ per cent disregarding absorption in the foil. This absorption reduces both F and τ_0 but the large difference between theory and experiment is mainly due to the nonuniform thickness of the foil. Variations in d up to several microns have been measured. These are sufficient to explain the low experimental values.

Similar results have been obtained with $d=40\ \mu$ foils and 2d grids of $g=40\ \mu$; first-order wavelength 161 μ, $F\simeq 10$, $\tau_0\simeq 50$ per cent. The theoretical properties are $F=16$ and $\tau_0=92$ per cent.

In Fig. 9 the measured properties of a FPI of the type of Section IV, 3) are compared with the theoretical calculations (13) and (14). This construction of a FPI yielded the highest F and τ_0 because of the absence of any substrate which would reduce the reflectivity of the grids and cause additional absorption. Nevertheless, both F and τ_0 reach only about 80 per cent of their theoretical values These reductions are again attributed to a small unevenness of the reflectors (see Appendix).

VI. Some Applications of FPI's

1) A simple application is the determination of the absorptivity of 2d grids from the peak transmission of a FPI. For this method of measuring the small quantity A it must be provided that the influence of nonuniform spacing is negligible. The grids have to be plane and parallel within about $0.1\lambda/(4nF)$ (see Appendix). Otherwise only an upper limit of A can be obtained. From our measurements on the FPI type of Section IV, 3) it follows, for example, that $A\leq 1.2$ per cent for a 2d-nickel grid of $g=50\ \mu$, $g/a=8$, $t=a$, at $\lambda=200\ \mu$. The theoretical value from (10) is $A=0.9$ per cent.

2) The FPI may be used as the dispersion element instead of a grating in a far infrared spectrometer. Using sufficiently small g and g/a, a resolution should be obtainable even in first order which is similar to the resolution of far infrared grating spectrometers. The problem of prefiltering against overlapping orders remains the same as with the grating. Jacquinot[16] showed, how-

[16] P. Jacquinot, "The luminosity of spectrometers with prisms, gratings, and Fabry-Perot etalons," *J. Opt. Soc. Am.*, vol. 44, pp. 761–765; October, 1954.

ever, that the FPI is capable of a considerably larger energy flux than a grating spectrometer of equal resolution and assuming equal areas of the FPI and the grating. In the far infrared the energy flux is mainly determined by the receiver. Therefore, a far infrared spectrometer of the Fabry-Perot type can be built more compact than an equivalent grating instrument.

An illustration of this spectroscopic application of the FPI is Fig. 10. The radiation of the mercury arc lamp L passed through the FPI (Fig. 5) and was received by a bolometer B. The upper part of Fig. 10 is the signal recorded when the first order wavelength of the FPI was tuned from 100 μ to 380 μ. The absorption of the atmospheric water vapor on the 5-meter path between source and receiver caused the numerous absorption lines. The positions of some H_2O rotational lines are indicated for comparison at the upper edge of the picture. The lower part of Fig. 10 is a simplified representation of the optical arrangement. The beams which are in fact reflected at the mirrors $M_1 \cdots M_4$ have been drawn unfolded for clarity. M_1 and M_4 are elliptical mirrors, and M_3 is a spherical one. The chopper Ch modulated the radiation with 12.5 cps to facilitate the amplification of the receiver signal. P is a 1.2-mm foil of black polyethylene which absorbs the visible and near infrared radiation. The remaining necessary prefiltering was not done in the conventional way by an absorption filter or by zero-order reflection at an echelette type filter grating. In obtaining the spectrum of Fig. 10, instead, the reflection characteristic of a 2d-metal grid was used for prefiltering. The radiation was reflected at the metallic mesh M_2 which has $g=108$ μ and $g/a=4.8$. Its reflectivity is large for $\lambda \gg g$ and has a minimum at $\lambda \simeq g$. ($R \simeq 1-T$, for T compare Fig. 2.) We found that for wavelengths shorter than this minimum wavelength the zero-order reflectivity seems to stay at a small level in contrast to the echelette filter grating. Further investigations are necessary on these optical properties of 2d grids at $\lambda < g$.

Another advantage of the 2d grid for prefiltering is the absence of polarization effects if the grid is used at normal incidence.

3) A tunable FPI is a simple device to check quantitatively the radiation purity and the efficiency of the prefiltering in a grating spectrometer. The spectrometer being set to the wavelength λ_0, its radiation also contains $\lambda_0/2$, $\lambda_0/3$, $\cdots$, if the prefiltering is insufficient. A FPI which is tuned in first order to one of these wavelengths is not transparent to λ_0. Thus, even small amounts of the undesired short-wavelength radiation are detectable quantitatively.

4) Another application of the FPI as a narrow-band filter is its use for separating the harmonics of a crystal harmonic generator. An example is Fig. 11[17]. The output of the harmonic generator was radiated from a horn antenna through a FPI and received by a bolometer. Here 1d grids could be used in the FPI for linearly polarized radiation. Fig. 11 shows the received signal vs the spacing of the grids. The different orders q of the third to seventh harmonic have been observed. The fundamental wavelength and the second harmonic were eliminated by a short piece of waveguide with suitable cutoff wavelength between the harmonic generator and the horn antenna.

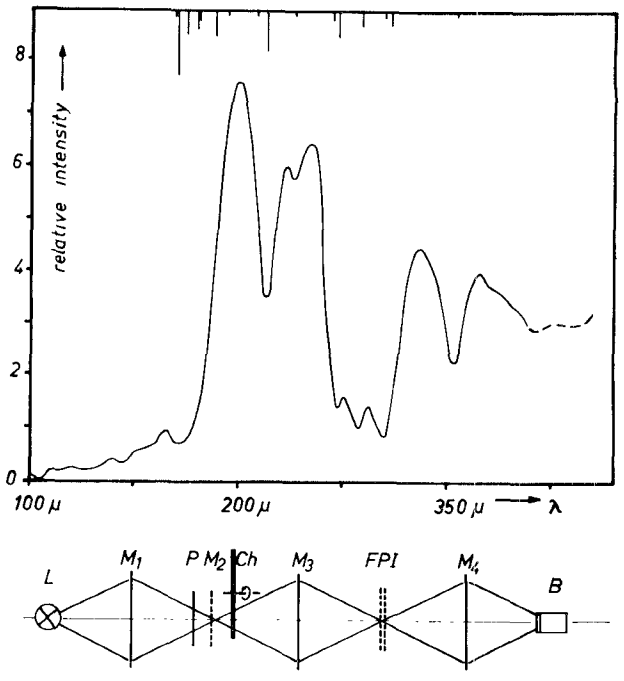

Fig. 10—Emission spectrum of the mercury arc with absorption lines of water vapor, obtained with FPI, and optical arrangement.

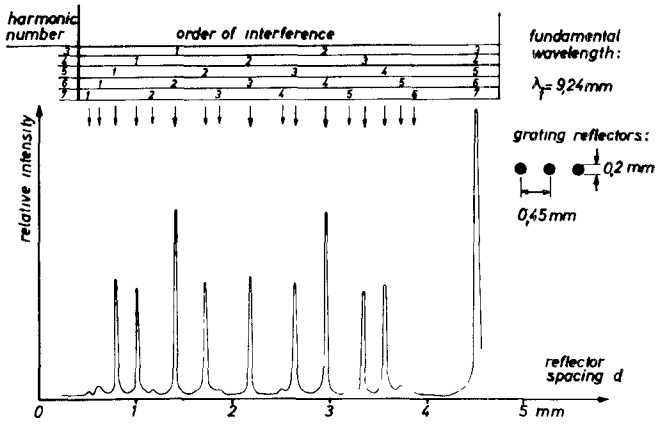

Fig. 11—Spectrum of a crystal harmonic generator, obtained with FPI with 1d grids.[17]

Appendix

The Influence of a Nonuniform Spacing

The spacing d is different from point to point of the surface of real FPI due to the unevenness of the reflectors as well as to the finite accuracy possible in adjusting their parallelism. Each sufficiently small area of

[17] Courtesy of H. Happ and E. Lux, to be published.

the FPI may be treated as a single FPI with plane and parallel reflectors. The whole FPI is composed of these single FPI's with different spacings. Its amplitude transmissivity is the averaged amplitude transmissivity of these single FPI's, each weighted with its fractional part of the whole surface area.

The resulting power transmission curve shows quantitatively the influence of the nonuniform spacing.

The decomposition in single FPI's and their treatment by the normal Airy formula is a good approximation if in each single FPI the angle α of inclination between the two reflectors is sufficiently small, namely,

$$\alpha^2 \ll \frac{25}{9F^3(5 + \ln F)^3} \cdot \tag{15}$$

This condition has been derived from a consideration of Born and Wolf.[18] We can estimate that it has been fulfilled at all q and F values of our experiments. With $F=30$, $q=10$, for example, (15) yields $\alpha<0.4\cdot10^{-3}$. Therefore, the treatment of the uneven FPI as a sum of single, even FPI's with different spacings is justified.

The power transmissivity of the single FPI may be expressed as

$$\tau(\delta) = \tau_0 \cdot H(\delta) \cdot H^*(\delta) \tag{16}$$

where

$$H(\delta) = (1 - R) \cdot (1 - \mathrm{Re}^{j\delta})^{-1}$$

is the normalized amplitude transmissivity. $H^*(\delta)$ is the conjugate complex of $H(\delta)$. The transmissivity is $\tau(\delta)=\tau_0$ if $\delta=2\pi q$ and drops to 0.5 τ_0 if $\delta-2\pi q=\pm\pi/F$. By this a normalized frequency x is defined,

$$x = (\delta - 2\pi q) \cdot F/\pi = 2F(2nd/\lambda - q - \phi/\pi). \tag{17}$$

In this scale the center of the transmission band lies at $x=0$ and the points of half-maximum intensity are $x_{1/2}=\pm1$. The function $H(\delta)$ may be approximated for $R\rightarrow1$ by

$$H_1(x) = (1 - jx)^{-1}. \tag{18}$$

Later on, this function will facilitate integration. $H_1(x)$ approximates $|H(\delta)|$ within 2 per cent and the phase of $H(\delta)$ within 20° in the region $R\geq0.8$ and $|x|\leq3$,that is, in the neighborhood of the transmission bands where $HH^*\geq0.1$.

Now the unevenness must be specified For mathematical simplicity it is assumed that all spacings d are equally frequent in the range

$$\bar{d} - b\lambda/(4nF) \leq d \leq \bar{d} + b\lambda/(4nF) \tag{19}$$

where b is the maximum deviation Δd from the mean spacing $\bar{d}$ measured in terms of $\lambda/(4nF)$,

$$b = \Delta d \cdot 4nF/\lambda. \tag{20}$$

[18] M. Born and E. Wolf, "Principles of Optics," Pergamon Press, New York, N. Y., p. 352; 1959.

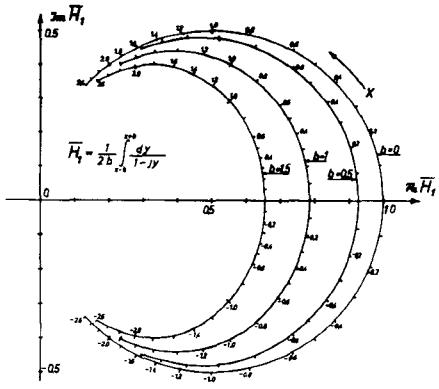

Fig. 12—Averaged transmissivity of a FPI: normalized amplitude transmissivity.

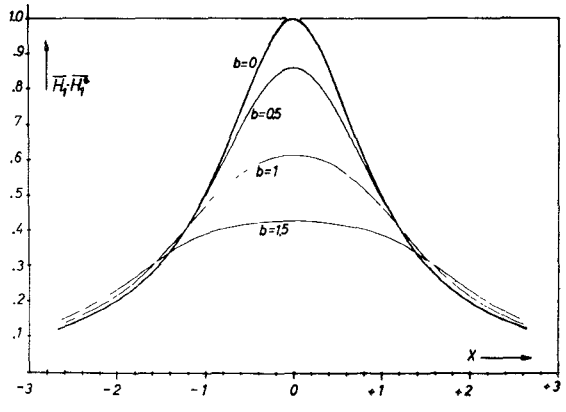

Fig. 13—Averaged transmissivity of a FPI: normalized power transmissivity.

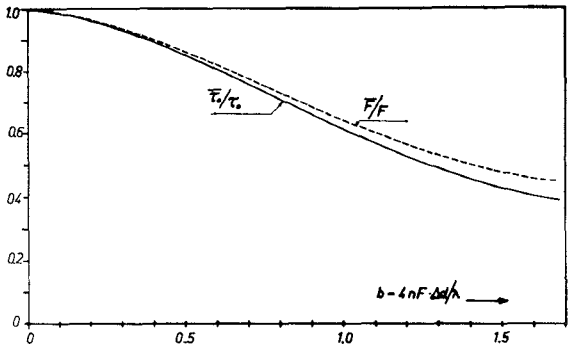

Fig. 14—Reduction of the properties of a FPI due to a nonuniform spacing.

Here n is the refractive index of the medium between the reflectors.

For this distribution of spacings the averaged amplitude transmissivity is

$$\overline{H} \simeq \overline{H}_1(x) = \frac{1}{2b} \arctan \frac{2b}{1 - b^2 + x^2} + j\frac{1}{4b} \ln\left(1 + \frac{4bx}{1 + (x - b)^2}\right) \tag{21}$$

where now for x in (17), d must be replaced by $\bar{d}$. This complex function is represented in Fig. 12 for various degrees of unevenness ($b=0$, 0.5, 1, 1.5). Fig. 13 is the

resulting power transmissivity $\overline{H}_1 \cdot \overline{H}_1^* = \bar{\tau}(x)/\tau_0$. A small unevenness is seen to reduce the transmissivity only in the center part of the transmission band ($b = 0.5$). A larger unevenness also affects its wings, they are slightly increased.

The peak transmission τ_0 of the ideal FPI is reduced by the unevenness to $\bar{\tau}_0$, and the bandwidth, measured between the points 0.5 $\bar{\tau}_0$, is increased from $2\pi/F$ to $2\pi/\overline{F}$ in the x scale. In Fig. 14 the ratios $\bar{\tau}_0/\tau_0$ and $\overline{F}/F$ are plotted vs b, the parameter of unevenness. The properties of the FPI remain essentially unchanged by an unevenness up to $b = 0.1$, that is up to $\Delta d \leq 0.1\lambda/(4nF)$. An unevenness of the order $\Delta d \simeq \lambda/(4nF)$ reduces, however, both F and τ_0 to approximately half their ideal values. It is remarkable that for a given unevenness F and τ_0 are reduced by nearly the same factor,

$$\overline{F}/F \simeq \bar{\tau}_0/\tau_0. \tag{22}$$

This fact is not determined by the special assumption (19) for the distribution of spacings. It results for all reasonable distributions if they are not too broad. The amplitude transmissivity is obtained by weighting $H_1(x)$ (see curve $b = 0$ in Fig. 12) with the distribution function. If the distribution is narrow, this averaging process reduces the center part of the transmission band and has negligible influence on the wings, as it was already observed for the special distribution (19). As a consequence the points $x_{1/2}$ of half-maximum intensity are shifted approximately along the power transmission curve of the ideal FPI which is the curve $b = 0$ in Fig. 13.

$$\tau(x)/\tau_0 \simeq H_1(x)H_1^*(x) = (1 + x^2)^{-1}. \tag{23}$$

The shift goes from $x_{1/2} = \pm 1$ to $\bar{x}_{1/2} = \pm(2\bar{\tau}_0/\tau_0 - 1)^{1/2}$ and results in a decrease of the finesse.

$$\frac{\overline{F}}{F} = \frac{x_{1/2}}{\bar{x}_{1/2}} = \frac{\bar{\tau}_0}{\tau_0} \cdot \left(2\frac{\bar{\tau}_0}{\tau_0} - \frac{\bar{\tau}_0^2}{\tau_0^2}\right)^{-1/2}. \tag{24}$$

The value of the last bracket is only slightly different from 1. It lies between 0.9 and 1 for $0.6 \leq \bar{\tau}_0/\tau_0 \leq 1$. Therefore, in good approximation (22) should hold for all reasonable distributions of spacing as long as this ratio (22) is ≥ 0.6.

A relation of the type (22) is observed between the experimental and theoretical values in Figs. 8 and 9. Using Fig. 14 the magnitude of the unevenness and of the error in parallelism is estimated to be $\Delta d = 1.5 \cdots 2\ \mu$ for both types of FPI's.

ACKNOWLEDGMENT

The authors are indebted to the editors for their comments and suggestions. They also wish to thank the Deutsche Forschungsgemeinschaft which has supported the construction of the grating spectrometer.

Spherical Mirror Fabry-Perot Resonators*

ROBERT W. ZIMMERER†, SENIOR MEMBER, IEEE

Summary—**An experimental investigation of the Fabry-Perot Interfometer (FPS) using spherical mirrors is reported. The FPS was operated as a microwave resonant cavity at 60 to 70 Gc. Measurements were made of the loss and coupling as a function of mirror spacing. The electric field variation within the resonator was also measured. Other characteristics of the spherical Fabry-Perot resonator were observed and are discussed.**

A qualitative discussion of the behavior of a spheroidal cavity resonator is presented and its relation to the FPS and beam waveguide is demonstrated.

INTRODUCTION

THE SPHERICAL mirror Fabry-Perot Interferomter (FPS) was first introduced as a new optical instrument by Connes [1]. In a series of papers [1], [2], he developed a geometrical optics theory and application of the instrument. With the advent of the laser the FPS was employed as a resonator and an electromagnetic theory of its operation was developed by several investigators at Bell Telephone Laboratories [3]–[7]. In a parallel development of the beam waveguide for the transmission of quasi-optical microwave power, Goubau and his associates have developed an electromagnetic theory [8] which has many applications to the FPS. The application and experimental verification of these various theories has been most rapid. The direct observation of laser output [9], the successful operation of the microwave FPS [10], [11], the transmission line studies of the beam waveguide [12]–[15], all verified the theoretical soundness of the work.

We have constructed and operated a variety of microwave Fabry-Perot resonators of both planar and spheri-

* Received April 29, 1963; revised manuscript received June 20, 1963. A preliminary note on this work has been published by the author, "Experimental investigation of Fabry-Perot interferometers," PROC. IRE (*Correspondence*), vol. 51, pp. 475–476; March, 1963.

† National Bureau of Standards, Boulder, Colo.